Supplemental Methods

CTAC Image Acquisition

In the training population, CTAC scans were performed free breathing without ECG-gating in helical mode acquired with the built-in Discovery 570c CT camera system (Lightspeed VCT 64, GE, Boston, USA) for patients undergoing nuclear imaging with either the NM530c and Discovery 570c. The acquisition parameters were adjusted by the technologists based on patients' body mass index (BMI). For patients with BMI <40 kg/m2, the following parameters were used: tube current: 60 mA, tube voltage: 120 kV, rotation time: 0.4 seconds, pitch: 0.98, number of slices: 89, helical slice thickness: 2.5 mm, slice spacing: 2.5 mm. For patient with BMI ≥40 kg/m2, similar parameters were used with adjusting the tube current to 150 mA.

In the first external site, CTAC imaging was performed after the rest acquisition during end-expiratory breath hold without ECG-gating, in helical mode with a slice thickness of 5-mm, tube voltage of 120 kV and 20 mA, using a 512x512 matrix. At the other external site, CTAC was acquired with prospectively ECG-triggered sequential images at 75% of the R-R interval, 2.5-mm section thickness, and 0.35-s gantry rotation times at 120 kV and 200–250 mA, depending on the patient's size and also 512x512 matrix.

Image Quality Control

Stress supine acquisitions were used for all analyses. Non-attenuation corrected (NC) and AC images were reconstructed on site prior to image de-identification *(8)*. Sites used proprietary reconstruction algorithms specific to the pinhole collimator design of the camera system. This algorithm includes resolution recovery but does not include scatter correction to the best of our knowledge. Correction of CTAC misregistration was performed at each site according to clinical protocols. De-identified image datasets were transferred to the core laboratory (Cedars-Sinai Medical Center) where quality control was performed by experienced technologists, including verification that complete image datasets were transferred and assessment of myocardial contours. Myocardial contours were generated in the testing set automatically with Quantitative Perfusion SPECT (QPS) /Quantitative Gated SPECT (QGS) software (Cedars-Sinai Medical Center, Los Angeles, CA). This was performed to allow for image quantification. Importantly, contours from QGS/QPS were not used in any way during DeepAC model training.

Model Architecture

Mean normalization was utilized to normalize the NC and AC images sets with the mean value of the NC images *(11).* In order to mitigate potential background artifacts, 32x32x32 volumes of interest centered on the left ventricle were used as the input *(11).* The generator model was similar to the Attention UNet 3D model *(12),* with instance normalization and discriminator similar to the pix2pix model *(13).* The generator includes 4 level 3D UNet along with an attention gate which combines the input from a lower level with the skipped connection and helps the generator to implicitly focus on relevant structures at a lower computational overhead as shown in Figure 1. The discriminator and the generator were trained together until Nash equilibrium was achieved similar to game theory, with no additional benefit to either the generator or the discriminator, so that the game remains in equilibrium. The cost function for the cGAN architecture included the standard GAN loss, along with absolute error between the DeepAC and AC and a perceptual loss *(14)* in the feature space for visual matching. The weights for the proposed architecture were initialized by Xavier initialization *(15)* and Adam optimizer *(16)* was used to linearly decay the learning rate to 0. Momentum of 0.5 and an initial learning rate of 0.0002 were set.

Supplemental Table 1: Characteristics of the training population.

Characteristic	Overall N = 4,886	Training N = 4,398	Validation N = 488	p-value
Age, median (IQR)	64 (56, 73)	64 (56, 73)	64 (57, 73)	0.5
Male, n (%)	2,705 (55)	2,437 (55)	268 (55)	0.8
BMI, median (IQR)	29 (26, 34)	29 (25, 34)	29 (26, 33)	>0.9
Past Medical History, n (%)				
Hypertension	3,204 (67)	2,875 (67)	329 (69)	0.4
Diabetes Mellitus	1,292 (27)	1,159 (27)	133 (28)	0.7
Dyslipidemia	2,649 (55)	2,360 (55)	289 (60)	0.024
History of CAD	873 (18)	789 (18)	84 (18)	0.7
Stress test type, n (%)				0.8
Exercise	1,775 (36)	1,595 (36)	180 (37)	
Pharmacologic	3,106 (64)	2,798 (64)	308 (63)	
Resting Heart Rate, median (IQR)	71 (63, 80)	71 (63, 80)	71 (63, 80)	0.2
Resting BP- Systole, median (IQR)	138 (124, 152)	138 (124, 152)	138 (125, 154)	0.8

Supplemental Table 1: Characteristics of the population used for model training and validation.

BMI – body mass index, CAD – coronary artery disease, IQR – interquartile range.

Supplemental Table 2

LAD (n = 41/604)	AUC (95% CI)	p-value
DeepAC TPD	0.77 (0.69 – 0.86)	Reference
AC TPD	0.80 (0.72 – 0.88)	0.367
NC TPD	0.69 (0.59 – 0.79)	0.007
LCX (n = 16/604)	AUC (95% CI)	p-value
DeepAC TPD	0.74 (0.60 – 0.88)	Reference
AC TPD	0.71 (0.57 – 0.86)	0.408
NC TPD	0.60 (0.45 – 0.76)	0.024
RCA (n = 22/604)	AUC (95% CI)	p-value
DeepAC TPD	0.76 (0.64 – 0.87)	Reference
AC TPD	0.72 (0.60 – 0.85)	0.464
NC TPD	0.70 (0.56 – 0.83)	0.217

Per-vessel diagnostic accuracy. AC – attenuation correction imaging, AUC – area under the receiver operating characteristic curve, CI – confidence interval, LAD – left anterior descending, LCX – left circumflex, RCA – right coronary artery, TPD – total perfusion deficit.

Supplemental Figure 1:

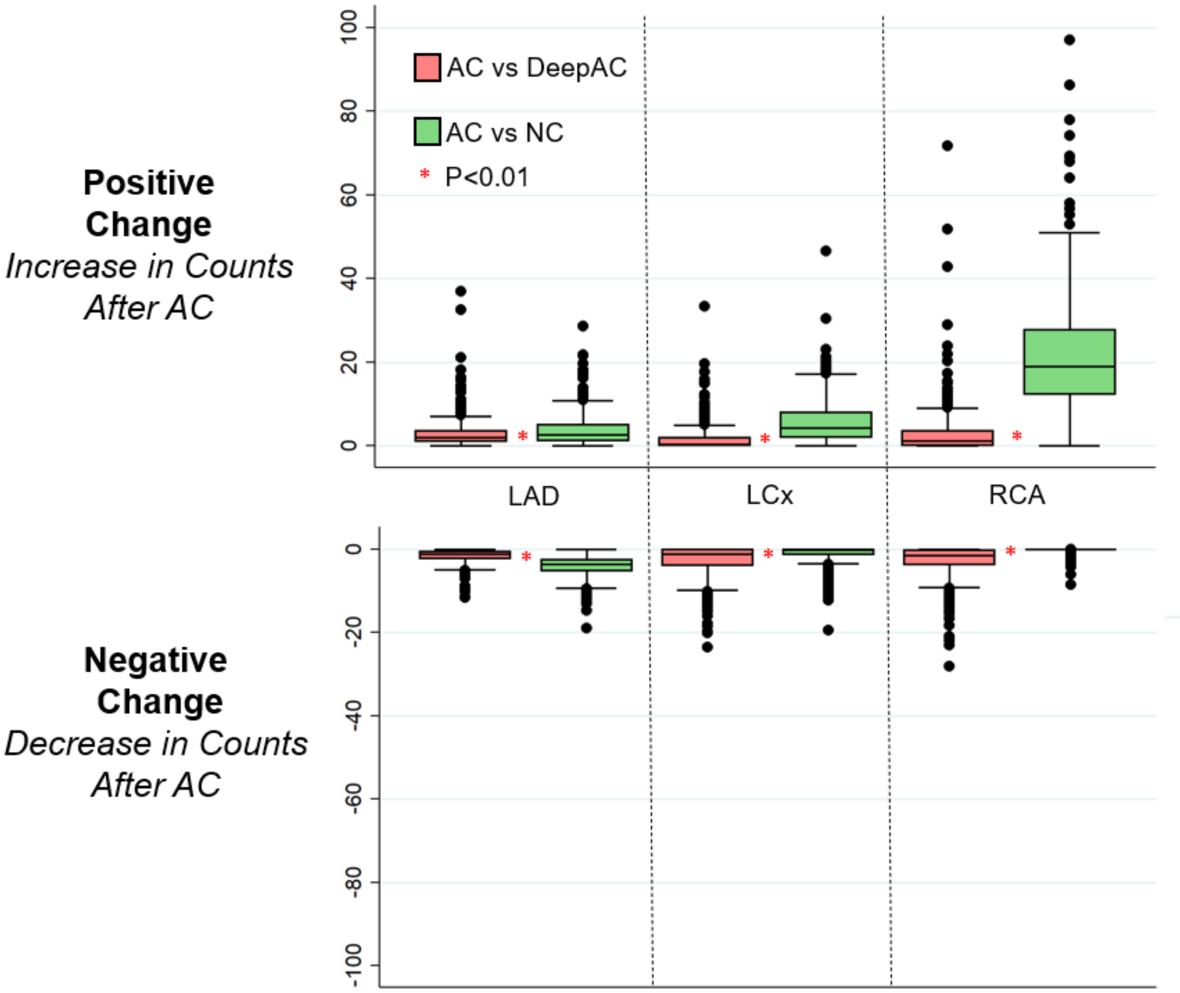

Change analysis (voxel-by-voxel analysis after subtraction of co-registered images). Actual attenuation corrected (AC) images were the reference image for comparisons of AC vs DeepAC (red) and AC vs non-attenuation corrected (NC) images (green).

Supplemental Figure 2:

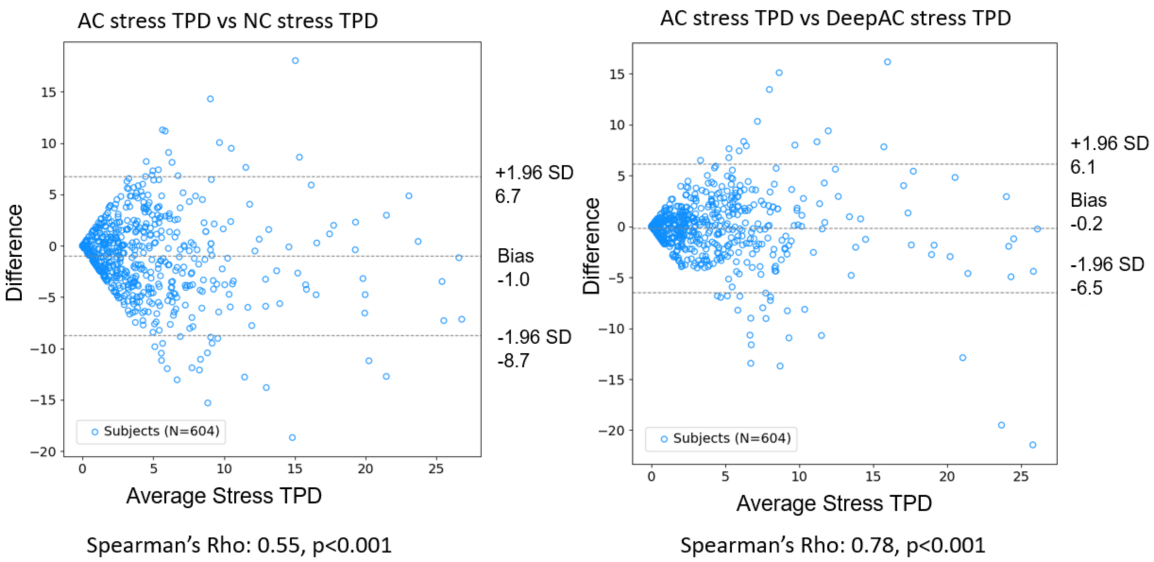

Bland-Altman Analysis outlining differences between stress total perfusion deficit (TPD). Limits of agreement were closer for attenuation corrected (AC) TPD vs DeepAC TPD compared to AC TPD vs non-attenuation corrected (NC) TPD ($p<0.001$).